

# Spin-dependent Cooper Pair Phase and Pure Spin Supercurrents in Strongly Polarized Ferromagnets

R. Grein, M. Eschrig, G. M. Staudis, and Gerd Schön

Institut für Theoretische Festkörperphysik and DFG-Center for Functional Nanostructures,  
 Universität Karlsruhe D-76128 Karlsruhe Germany  
 (dated: February 21, 2024)

We study heterostructures of singlet superconductors (SC) and strongly spin-polarized ferromagnets (sFM) and show that a relative phase arises between the superconducting proximity amplitudes in the two ferromagnetic spin bands. We find a tunable pure spin supercurrent in a sFM contacted with only one SC electrode. We show that Josephson junctions are most effective for a spin polarization  $P = 0.3$ , and that critical currents for positive and negative bias differ for a high transmission Josephson junction, due to a relative phase between single and double pair transmission.

PACS numbers: 72.25.Mk, 74.50.+r, 73.63.-b, 85.25.Cp

Superconductor (SC)/ferromagnet (FM)-hybrid structures have triggered considerable research activities in recent years [1, 2, 3, 4, 5, 6, 7, 8, 9, 10, 11]. In particular, FM Josephson junctions are promising spintronics devices as they allow for tuning the critical current via the electron spin. However, due to the competition between the uniform spin alignment in the FM and spin-singlet pairing in the SC, singlet superconducting correlations decay in the FM on a much shorter length scale than in a normal metal [12]. Although this results in a rapidly decaying Josephson current for long junctions, the proximity effect leads to interesting physics in short and/or weakly polarized junctions, e.g., oscillations of the supercurrent as a function of the thickness of the interlayer that can give rise to  $\pi$ -junction behavior [12, 13]. Recently however, in contradiction with these expectations, long-range supercurrents have been reported through strongly spin-polarized materials [6]. Theoretical calculations have shown that for strongly polarized ferromagnets (sFM) spin scattering at SC/FM interfaces [14] leads to a transformation of singlet correlations in the SC into triplet correlations [3] (the 'triplet reservoirs' of Ref. [9]), that can carry a long-range supercurrent through the sFM [3, 7, 8, 9, 10, 11].

So far, transport calculations in SC/FM hybrids have mostly concentrated on either fully polarized FMs, so-called half metals (HM), or on the opposite limit of weakly polarized systems. However, most FMs have an intermediate exchange splitting of the energy bands of the order of 0.2-0.8 times the Fermi energy  $E_F$ . For this intermediate range, one could naively expect a behavior similar to two shunted half-metallic junctions. We will show, using a microscopic interface model, that this picture is inadequate, and point out the crucial role played by the interfaces in coupling the sFM spin bands.

In this work, we study Josephson junctions with a strongly polarized interlayer, and find fundamental differences compared to both half-metallic and weakly polarized interlayers. In particular, we see that although correlations between  $\uparrow$ - and  $\downarrow$ -electrons are suppressed

due to the strong exchange field, spin-active interfaces generate interactions between long-range triplet supercurrents in the two spin bands. We find that the long-range critical Josephson current varies non-monotonously with spin polarization  $P$ , showing a maximum around  $P = 0.3$ . Furthermore, additional phases arising from the interfaces [14], especially when the exchange splitting is strong, lead to different current-phase relations for the spin-resolved currents  $I_{\uparrow}$  and  $I_{\downarrow}$  through the junction. We show how this gives rise to (i) a relative phase between single pair and "crossed" two-pair transmission; the latter process is illustrated in Fig. 1a, with equal numbers of pairs transferred in the  $\uparrow$  and  $\downarrow$  band; (ii) different critical Josephson currents for opposite bias; (iii) equilibrium shifts in the current phase relation, in contrast to previous predictions [9]; and (iv) a tunable spin supercurrent in a FM brought into contact with a single SC electrode; we propose an experiment to measure this remarkable effect.

Quasiclassical Green's functions (QCGF) [15, 16] are a powerful tool to describe hybrid structures of superconductors and non-superconducting materials. Consider, e.g., the interface between a SC and a sFM shown in

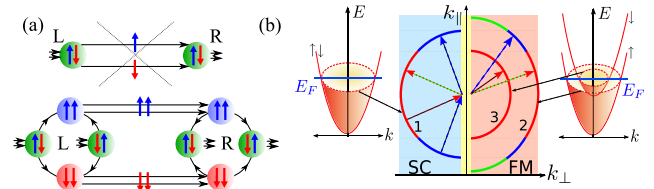


FIG. 1: (color online) (a) The coherent transfer of singlet pairs via a sFM (top) is not possible. However, the "crossed" pair transmission process (bottom) is possible and leads to intriguing effects in high transmission junctions. (b) SC/sFM interface, showing the Fermi surfaces on either side (thick lines). Assuming momentum conservation parallel to the interface ( $k_{\parallel}$ ), a quasiparticle incident from the SC can either scatter into two (dotted arrows), or into only one (dashed arrow) spin band of the FM.

Fig. 1b. For trajectories on the SC side, labeled 1, and characterized by Fermi momentum  $p_{F1}$  and Fermi velocity  $v_{F1}$ , the QCGF is obtained from the microscopic one,  $\hat{G}$ , by integrating out the components oscillating on the Fermi wave length scale  $\xi_{F1} = \hbar/v_{F1}$ :  $\hat{g}(p; R; \omega; t) = \int d p \hat{G}(p; R; \omega; t)$ , where  $p = v_{F1}(p - p_{F1})$ . The QCGF,  $\hat{g}$ , then varies as a function of the spatial coordinate  $R$  at a scale set by the superconducting coherence length  $\xi_0 = \hbar/v_{F1} = 2 k_B T_c$ , and obeys the Eilenberger equation

$$i\hbar v_{F1} \frac{\partial}{\partial R} \hat{g} + [\hat{\tau}_3 \hat{g} - \hat{h}; \hat{g}] = 0; \quad (1)$$

with normalization condition  $\hat{g}^2 = -2\hat{1}$  [16]. Here, the hat denotes the  $2 \times 2$  Nambu matrix structure in particle-hole space and  $\hat{\tau}_3$  is the third Pauli matrix;  $\hat{h}$  includes all mean field and self energy terms governing the quasiparticle motion along QC trajectories aligned with  $v_{F1}$ , and labeled by  $p_{F1}$ ;  $\hat{\tau}_3$  is the SC order parameter.

The exchange field  $J_{FM}$  in a sFM is comparable to the Fermi energy. As opposed to the weak polarization limit ( $J_{FM} \ll E_F$ ) this cannot be described by a term  $J_{FM} \sim$  (with  $\sim$  the vector of Pauli spin matrices) in  $\hat{h}$  of Eq. (1), because the QC approximation in this case neglects terms of order  $J_{FM}^2/E_F$  compared to  $E_F$ . In most SCs, this is not justified for  $J_{FM} > 0.1E_F$ . However, for sufficiently large  $J_{FM} \sim E_F$  the coherent coupling of the spin bands in the FM can be disregarded. Consequently, we define an independent QCGF for each spin band  $f_{2,3}$  in Fig. 1b:  $\hat{g}(p; R; \omega; t) = \int d p \hat{G}(p; R; \omega; t)$ ; where  $p = v_F(p - p_F)$ . The exchange field is incorporated by the different Fermi velocities  $v_F$  and momenta  $p_F$  in the two spin bands, and does not enter the equation of motion (1) for the QCGFs. The  $\hat{g}$  are Nambu matrices with diagonal (g) and off-diagonal (f) components. These components are spin scalar, as opposed to the QCGF in the SC where they form a  $2 \times 2$  spin matrix as a result of spin coherence. Indeed, the spins of the pair wavefunction in the FM are fixed either to  $\uparrow\uparrow$  (band 2 in Fig. 1b) or to  $\downarrow\downarrow$  (band 3).

The interface enters the QC theory in the form of effective boundary conditions [17, 18, 19] connecting the incident and outgoing QCGFs for the three Fermi surface sheets  $f_{1,2,3}$ . The boundary conditions are subject to kinetic restrictions [20], as illustrated in Fig. 1b. Note that, for a sFM, all singlet correlations are destroyed within the interface region (they decay on the short length scale  $\xi_j = \hbar/(p_{F2} - p_{F3}) \sim \hbar/v_{F2,3} = \xi_0$  [21]). The boundary conditions are formulated in terms of the normal-state scattering matrix (S-matrix) of the interface [19], which for three bands has the general form

$$\hat{S} = \begin{matrix} & \begin{matrix} 2 & 3 \end{matrix} \\ \begin{matrix} \hat{R}_{11} \\ 4 \hat{T}_{21}^T \\ \hat{T}_{31}^T \end{matrix} & \begin{vmatrix} \hat{T}_{12} & \hat{T}_{13} \\ r_{22} & r_{23} \\ r_{32} & r_{33} \end{vmatrix} \end{matrix} \begin{matrix} \hat{v}_j \\ \hat{v}_j \\ \hat{v}_j \end{matrix}; \quad \hat{v}_j = \begin{matrix} 2 & 3 \\ \hat{v}_j^+ & \hat{v}_j^- \\ \hat{v}_j^+ & \hat{v}_j^- \end{matrix} \begin{matrix} 0 & 0 \\ e^{i\frac{\omega}{2}} & 0 \\ 0 & e^{i\frac{\omega}{2}} \end{matrix} : \quad (2)$$

We obtain the reflection and transmission coefficients from a microscopic calculation. We consider an interface

formed by a thin ( $\xi_F$ ) insulating FM layer of thickness  $d$  between the SC and bulk sFM (yellow areas in Figs. 1b and 2a), characterized by an interface potential  $V_I = J_I \sim$ . The orientation of the exchange field  $J_I$  in the interface layer is determined by angles  $\theta$  and  $\theta'$ , with the angle between  $J_I$  and the exchange field  $J_{FM}$  of the bulk sFM (see Fig. 2b). The S-matrix connecting incoming and outgoing amplitudes in the bulk SC and sFM is then obtained by a wave-matching technique, where the amplitudes in the interface layer are eliminated. Doing so, we obtain in the tunneling limit an S-matrix of the form  $\hat{R}_{11} = e^{i(\theta=2)\phi}$  [22],  $\hat{T}_{12} = \hat{T}_{21} = (t_2 e^{i\theta=2}; t_2^0 e^{i\theta=2})^T$  and  $\hat{T}_{13} = \hat{T}_{31} = (t_3^0 e^{i\theta=2}; t_3 e^{i\theta=2})^T$ . The spin mixing  $\theta$ -angles in these expressions [3, 14, 19] (also called spin-dependent interfacial phase shifts [23]), and all remaining S-matrix parameters are obtained from a microscopic calculation as outlined above. As such, they depend on  $d$ ,  $V_I$ ,  $\theta$ ,  $\theta'$ , and the Fermi momenta of the three bands (we assume  $j_{Ij} = j_{FM}$ ). The dependence on the angle  $\theta'$  is made explicit in Eq. (2), while the dependence on the angle  $\theta$  is implicit in the  $r$  and  $t$  parameters via  $t_{2,3}^0 / \sin(\theta=2)$ ,  $t_{2,3} / \cos(\theta=2)$  and  $r_{23}; r_{32} / \sin$ . In the following we use these tunneling-limit expressions to gain insight into the physics of the problem. The results shown in the figures however, are obtained by a full numerical calculation. For definiteness, we present results for parabolic electron bands with equal effective masses.

Applying these boundary conditions to a Josephson junction depicted in Fig. 2a, and assuming bulk solutions for the QCGFs incoming from the SC electrodes, we arrive at the following system of linear equations for the  $f$ -functions in the tunneling limit (labels  $k; j \in \{L, R\}$  with  $j \neq k$  denote the left/right interfaces):

$$\begin{matrix} f_2^{\text{out}} \\ f_3^j \end{matrix} = \begin{matrix} \hat{J}_{22} \hat{J} \\ 32 \hat{J}_{33} \hat{J} \end{matrix} \begin{matrix} 23 \\ j \end{matrix} \begin{matrix} 2 f_2^{\text{out}} \\ 3 f_3^k \end{matrix} + \begin{matrix} A_{12} \\ A_{13} \end{matrix} : \quad (3)$$

Here, the factors  $\hat{J} = e^{2j\theta} \hat{J} = v_j$ , where  $L = J$  is the junction length,  $\theta_n = (2n+1)k_B T$  the Matsubara frequency,  $v_j$  the Fermi velocity component along the interface normal, and  $f_{2,3}$  the band index, arise from the decay of the  $f$  functions in the sFM layer. As depicted in Fig. 2a, coupling between the sFM spin bands is provided by the quantity (for our model  $r_{23}r_{32}$  is real)

$$[r_{23}]_j = r_{23}r_{32} e^{i2\theta'} = [r_{32}]_j; \quad (4)$$

while the inhomogeneity in Eq. (3),  $[A_1]_j$ , can be interpreted as a pair transmission amplitude from the SC into spin band  $j$  of the sFM through the interface  $j$ . It reads

$$[A_1]_j = i \frac{\text{sgn}(\theta_n) \hbar}{1 - 2} (B + C) t^0 e^{i(\theta')} \begin{matrix} i \\ j \end{matrix} \quad (5)$$

$$B = \frac{+}{-} = \theta_n; \quad C = \frac{j\theta}{-} = \theta_n \quad (6)$$

$$= \sin \theta \sin(\theta - \theta'); \quad = \sin(\theta=2) = \theta_n \quad (7)$$

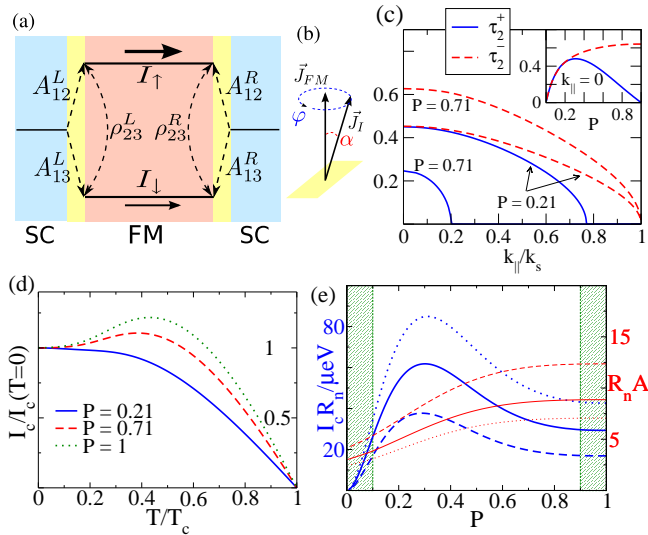


FIG. 2: (color online) (a) Josephson-junction with spin-active SC/sFM interfaces formed by magnetized layers (yellow). (b) Orientation of the interface magnetization described by spherical angles  $\theta$  and  $\alpha$ . (c) The quantities  $\tau_2^\pm$  in Eq. (7) vs.  $k_{||}/k_s$  for two polarizations  $P$ , and vs.  $P$  for perpendicular impact (inset). (d) Critical current  $I_c$  vs. temperature  $T$  for various polarizations  $P$  of the sFM layer. (e)  $I_c R_n$ -product and normal state resistance  $R_n A$  as function of  $P$  for  $T = 0.5T_c$ ,  $d = 0.25$ , and  $(V_L - V_R) = E_F = 10^4$  (dotted), 0.2 (full), 0.5 (dashed).  $R_n A$  in units of  $(e^2 N_{F1} V_{F1})^{-1}$ ,  $N_{F1}$  being the normal state SC DOS.  $\mu = 1.76$  meV. In all plots:  $\rho_L = \rho_R = 2$ ,  $\rho_L = \rho_R$ ,  $L = 0$ ,  $d = 0.5$ ,  $V_L - V_R = 0.5 E_F$ ,  $P_2 = 1:1.8 P_1$ , unless stated otherwise.  $P$  is tuned by  $P_3$ .

where  $\tau_n = P \frac{\tau_n^2}{\tau_n^2 + 2}$ ,  $\tau_n$  is the order parameter phase of the corresponding SC, and the  $+$  ( $-$ ) sign in  $\tau_n$  corresponds to  $\tau_n = 2$  (3). Note that  $\tau_n^0 / \sin(\tau_n)$ , implying that the generation of triplet correlations relies on  $\tau_n \neq 0$ .

In Fig. 2c we show  $\tau_2^\pm$ , Eq. (7), for the majority spin band ( $\tau = 2$ ) as a function of  $k_{||}$ . For large enough  $k_{||}$ ,  $\tau_2^+$  vanishes in contrast to  $\tau_2^-$ . This region of  $k_{||}$ -values allows for transmission into only a single spin band of the FM (see Fig. 1b). With increasing spin polarization  $P = (p_{F2} - p_{F3}) / (p_{F2} + p_{F3})$  it extends over a larger range of  $k_{||}$ -values, eventually spanning the entire Fermi surface for a half-metal. At the same time the maximal value of  $\tau_2^+$  decreases to zero, as demonstrated in the inset in Fig. 2c, where the parameters  $\tau_2^\pm$  are shown for normal impact as function of  $P$ . The different temperature ( $T$ ) dependencies due to the additional  $j_n^j$  term in Eq. (7). This interplay leads to an intriguing change in the  $T$ -dependence of the Josephson current, plotted in Fig. 2d. For high  $P$ , a non-monotonic behavior is observed similar to that for a HM [3, 11], due to the dominant  $C_2$  term, whereas for smaller  $P$  the term arising from  $B_2$  leads to a monotonic decay with increasing  $T$ . As a result, the bump in  $I_c(T)$  disappears with decreasing polarization.

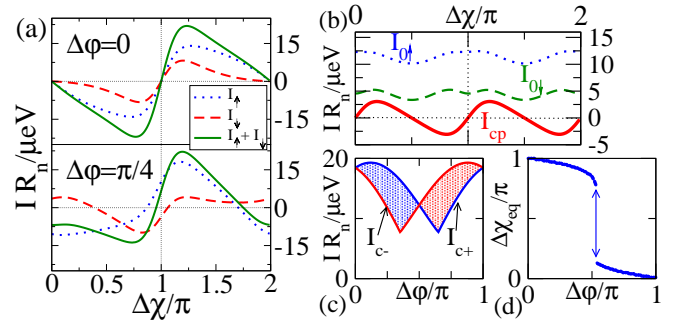


FIG. 3: (color online) (a) Spin resolved and total CPR for  $\Delta\phi = 0$  and  $\Delta\phi = \pi/4$ . (b) Coefficients  $I_{cp}$  and  $I_0$  of Eq. (8) vs.  $\Delta\chi/\pi$ . (c) Critical current in positive ( $I_{c+}$ )/negative ( $I_{c-}$ ) bias direction vs.  $\Delta\chi/\pi$ . (d) The equilibrium phase difference  $\Delta\chi_{eq}$  vs.  $\Delta\phi/\pi$  varies from  $\pi$  to 0. In all plots  $T = 0.2 T_c$ ,  $d = 0.25$ ,  $P_1 = 1$ ,  $P = 0.21$ , other parameters as in Fig. 2.

In Fig. 2e we plot the  $I_c R_n$  product as a function of  $P$  (left scale). The variation of the normal state resistance  $R_n$  with  $P$  (right scale) cannot account for the variation of  $I_c$ . The critical current is suppressed for small  $P$  due to small spin mixing angles (see Fig. 2c), and for high  $P$  due to reduction of conductivity in the minority spin band. We thus predict a maximum critical current in a sFM junction for intermediate  $P \approx 0.3$ . We caution that in the hatched regions in Fig. 2e, there are additional processes, not included in our model; e.g., for small  $P$  spin coherence leads to singlet amplitudes in the FM.

We now discuss intriguing effects associated with the angles  $\theta_{L,R}$  [see Eqs. (4-5) and Fig. 2b]. In Fig. 3a we plot the spin-resolved current-phase relation (CPR) [24] for a high transparency junction ( $d = 0.25$ ) as a function of  $\Delta\chi = \theta_R - \theta_L$  for two values of  $\theta = \theta_R = \theta_L$  [26]. Clearly, there is a non-trivial modulation of the CPR in the presence of  $\theta$ . We find that the CPR can be well described by the leading Fourier terms in  $\Delta\chi$ ,

$$I = I_{cp} \sin(\Delta\chi) + I_0 \cos(\Delta\chi) \quad (8)$$

where  $I_{cp} = I_{cp}(\theta)$  for spin  $\tau$  (#). Here,  $I_0$  (shown in Fig. 3b) and  $I_{cp}$  are renormalized due to multiple transmission processes. The first term in Eq. (8) describes a special type of multiple transmission process, which we call "crossed pair" (cp) transmission, shown in Fig. 1a. It is a result of singlet-triplet mixing and triplet rotation induced by the interfaces. Here two singlet Cooper pairs are effectively recombined coherently into two triplet pairs that propagate in different spin bands. Similar processes recombining a higher (but even) number of pairs will also contribute. The phase associated with these processes comes from  $[A_{12} A_{13}]_L [A_{12} A_{13}]_R$  factors with  $A_1$  from Eq. (5), and is given by multiples of  $(\theta + \theta') + (\theta - \theta') = 2\theta$ . Consequently,  $I_{cp}$  is independent of  $\theta$  and  $\theta'$ -periodic in  $\Delta\chi$ , as shown in Fig. 3b (full line). It is also obvious that  $I_{cp}$  is spin

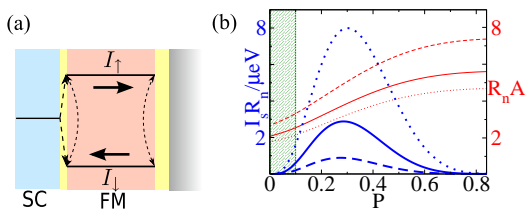


FIG. 4: (color online) (a) Setup with only one SC electrode. (b) Spin-supercurrent  $I_s$  vs.  $P$  for various  $(V_T - J_t) = E_F = 10^{-4}$  (dotted), 0.2 (full), 0.5 (dashed).  $R_n A$  refers to the normal state resistance of the SC/FM interface.  $d = \xi_{F1}$ , other parameters as in Fig. 2.

symmetric, i.e., it carries a charge current, but no spin current. We find that transfer processes with even number of pairs, but non-zero total spin, are in contrast to the spin transmission strongly suppressed. Contributions to the second term in Eq. (8) come from processes that transmit one more Cooper pair in one of the spin bands compared to the other, including single pair transmission. It is therefore spin-dependent in magnitude (see Fig. 3b) and shows  $\pi$  phase shifts with opposite signs for opposite spins. The relative phase between the two terms in Eq. (8) leads to surprising measurable effects for finite  $\phi$  and intermediate  $P$ . First, we find a difference in the positive ( $I_{c+}$ ) and negative ( $I_{c-}$ ) bias critical charge currents, as shown in Fig. 3c. This is also directly visible in Fig. 3a, where the maximum and minimum current have a different absolute value. Second, we find a shift of the equilibrium phase  $\phi_{eq}$  for the charge current, as shown in Fig. 3d (the jump as function of  $\phi$  is associated with multiple local free energy minima). We note that in the tunneling limit, Eq. (8) reduces to  $I_s = I_0 \sin(\phi + \pi/2)$ , and the equilibrium phase shift is present as long as  $I_0 \neq 0$ .

Another remarkable consequence of a non-zero  $\phi$  is observed for a setup shown in Fig. 4a, when an sFM is coupled via a spin-active interlayer to a single SC on the left, and is terminated by a magnetic surface on the right. All quasiparticles are reflected at the surface, leading to a zero charge current. However, not all quasiparticles are reflected back into their original spin band since spin-flip reflections [23 in Eq. (4)] mediate interactions between the two spin bands, and, remarkably, a pure spin supercurrent remains. In this case, both terms in Eq. (8) vanish as they are related to direct transmission. Instead, the leading term for the spin supercurrent is of second order in  $\phi$ ,  $I_s \propto \sin(2\phi)$ , resulting from the phases picked up when a triplet Cooper pair reflects at the right interface [25]. The maximal spin-current, defined as  $I_s = \max_{\phi} I(\phi)$ , is plotted in Fig. 4b as a function of spin polarization. Note that it vanishes both for  $P = 0$  and  $P = 1$ , since it requires the presence of two bands, and is maximum for intermediate  $P$ .

This pure spin current can be tuned by an external

microwave field that couples to the magnetization of the right surface in Fig. 4a, and thus leads to a time dependent  $\phi(t)$ . A high degree of control can be achieved by manufacturing a surface layer using a different magnetic material, preferably magnetized perpendicular to the bulk FM, thus optimizing external tunability. As  $\phi(t)$  acts as a time dependent superconducting phase, we predict in addition to a spin accumulation in the FM a measurable spin supercurrent, analogously to the ac charge Josephson current in a voltage biased junction.

In summary, we have presented a study of heterostructures between singlet superconductors and strongly spin-polarized ferromagnets. We have found that the Josephson effect markedly differs from that for a fully polarized material or for a ferromagnet with a weak spin band splitting. We discussed the importance of the phase-shift between single pair and "crossed" two-pair transfer processes that leads to measurable anomalous junction behavior. We have also found that a pure spin supercurrent is induced in a strongly polarized ferromagnet coupled to one singlet superconducting electrode, and have proposed a way of measuring this effect.

We thank T. Lofwander for stimulating discussions.

- 
- [1] F. S. Bergeret et al, Rev. Mod. Phys. 77, 1321 (2005).
  - [2] A. I. Buzdin et al, Rev. Mod. Phys. 77, 935 (2005).
  - [3] M. Eschrig et al Phys. Rev. Lett. 90, 137003 (2003).
  - [4] A. F. Volkov et al, Phys. Rev. Lett. 90, 117006 (2003).
  - [5] J. Kopp et al, Phys. Rev. B 69, 094501 (2004).
  - [6] R. S. Keizer et al, Nature 439, 825 (2006).
  - [7] M. Eschrig et al, J. Low Temp. Phys. 147, 457 (2007).
  - [8] M. Houzet et al, Phys. Rev. B 76, 060504(R) (2007).
  - [9] V. Braude and Yu. Nazarov, Phys. Rev. Lett. 98 (2007).
  - [10] Y. Asano et al, Phys. Rev. Lett. 98, 107002 (2007).
  - [11] M. Eschrig et al, Nature Phys. 4, 138 (2008).
  - [12] V. Buzdin et al, Pis'ma Zh. Eksp. Teor. Fiz. 35, 147 (1982); Z. Radovic et al, Phys. Rev. B 68, 014501 (2003).
  - [13] V. V. Ryazanov et al, Phys. Rev. Lett. 86, 2427 (2001); T. Kontos et al, Phys. Rev. Lett. 89, 137007 (2002).
  - [14] T. Tokuyasu et al, Phys. Rev. B 38, 8823 (1988).
  - [15] A. Schmid and G. Schon, J. Low Temp. Phys. 20, 207 (1975); J. W. Serene et al, Phys. Rep. 101, 221 (1983).
  - [16] G. Eilenberger, Zh. Eksp. Teor. Fiz. 55, 2262 (1968); A. I. Larkin and Y. N. Ovchinnikov, Zh. Eksp. Teor. Fiz. 55, 2262 (1968).
  - [17] A. Shelankov, J. Low Temp. Phys. 60, 29 (1985); A. Shelankov and M. Ožana, Phys. Rev. B 61, 7077 (2000).
  - [18] M. Eschrig, Phys. Rev. B 61, 9061 (2000).
  - [19] A. M. Iľlis, D. Rainer, and J. A. Sauls, Phys. Rev. B 38, 4504 (1988); M. Fogelstrom, ibid. 62, 11812 (2000); E. Zhao et al, ibid. 70, 134510 (2004).
  - [20] I. Zutic and O. T. Valls, Phys. Rev. B 61, 1555 (2000); K. Halteman and O. T. Valls, ibid. 66, 224516 (2002); J. Linder and A. Sudb, ibid. 75, 134509 (2007).
  - [21] The condition for treating the singlet components within QC theory is  $\frac{2}{j} \ll \frac{2}{F}$ .
  - [22] With a proper choice of the quantization axis in the SC, the reflection matrix  $\hat{R}_{11}$  is spin-diagonal.
  - [23] A. B. Rataas et al, Phys. Rev. Lett. 84, 2481 (2000); D. Huertas-Hemando et al, ibid. 88, 047003 (2002); A. C. Otter and W. Belzig, Phys. Rev. B 72, 180503 (2005).

[24] A. A. Golubov et al., Rev. Mod. Phys. 76, 411 (2004).

[25] A similar effect, however involving triplet superconductors with a FM interlayer has been reported in P. M. R. Brydon, D. Manske arXiv:0901.4096.

[26] Our final results only depend on  $\theta = \theta_R - \theta_L$ , in accordance with global spin rotational invariance.